Quadric Fitting for Handle Identification

Shiloh Curtis

***Abstract*—For robots to expand their capabilities to a wider range of manipulation tasks, it is important to identify grasps that are not just stable but have some other useful feature. In particular, most tools have handles, which afford stable grasping in such a way that the operational end of the tool can be easily used. Due to the geometry of the human hand, many handles can be approximated using quadric surfaces such as cylinders and ellipsoids. Quadrics can also be quickly and accurately fitted to point clouds. The quadric-based handle identification approach fits quadrics to objects, then tests them for handle-like characteristics; the centers of quadrics that pass these tests are likely to cluster around actual object handles. While this method did not perform well on all tested objects, on the majority of objects it achieved good results, with reasonable robustness to added synthetic noise.**

I. Introduction

Although the problem of robustly picking and placing objects is currently a major focus of robotics manipulation research, there are many other types of manipulation problems. In order to perform useful tasks, it is often important for robots to be able to pick up and use tools that they find in the world. This is a more strict requirement than simply finding a stable grasp; the grasp needs to be in a location such that the working end of the tool is usable.

Therefore, there has already been some effort towards finding useful places to grasp objects, based on the task for which they are to be used. Reference [1] used motion-capture to collect data on how humans grasp objects for different purposes, then trained a machine-learning model that attempted to transfer this to new objects.

However, in most cases, it is sufficient to grab an object by the handle, and most handles come in a few fairly consistent shapes: cylinder, ellipsoid, hyperboloid of one sheet. Because of the way the human hand is shaped, this is a popular grasping affordance.

II. Prior Work

Prior work [2] has used cylinder fitting to find grasp affordances on objects. I advance this work by using additional kinds of quadric surfaces, and by testing response to point clouds with artificially added noise.

III. Notes on Quadrics

Cylinders, ellipsoids, and hyperboloids of one sheet (the three "handle" shapes I use) are all categorized as quadrics, so it is important to first describe some of the mathematical properties of quadric surfaces.

A. Definitions

A quadric in three dimensions is any surface that can be defined by a second-degree polynomial in x, y, and z. The general equation for a quadric has the form

$$\begin{aligned} f(x,y,z) = Ax^2 + By^2 + Cz^2 \\ + 2Dxy + 2Exz + 2Fyz \\ + 2Gx + 2Hy + 2Iz + J = 0, \end{aligned}$$

where the coefficients $A \dots J$ are all real. It is useful to define two symmetric matrices based on this equation:

$$\mathbf{Q} = \begin{bmatrix} A & D & E & G \\ D & B & F & H \\ E & F & C & I \\ G & H & I & J \end{bmatrix}, \quad \mathbf{q} = \begin{bmatrix} A & D & E \\ D & B & F \\ E & F & C \end{bmatrix}$$

Given a point $\mathbf{x} = (x, y, z) \in \mathbb{R}^3$, the distance from $\mathbf{x}$ to the quadric is

$$d_q(\mathbf{x}) = [\mathbf{x}^T 1]\mathbf{Q}[\mathbf{x}^T 1]^T$$

and $\mathbf{x}$ lies on the quadric if $d_q(\mathbf{x}) = 0$.

B. Types of Quadrics

As laid out in [3, pp. 117-128], there are seventeen types of quadric surfaces, but the three that are relevant to the topic of handle fitting are the real ellipsoid, the hyperboloid of one sheet, and the real elliptic cylinder, these being the only "handle-shaped" quadrics. These surfaces can also be stably grasped at the center.

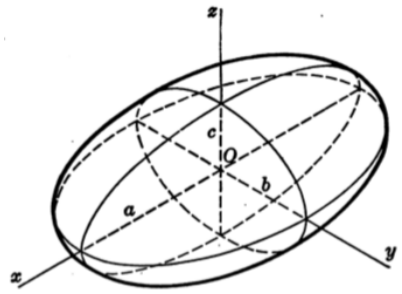

Fig. 1: Real ellipsoid, showing the semi-axes [3, p. 117].

The canonical form for the real ellipsoid is

$$\frac{x^2}{a^2} + \frac{y^2}{b^2} + \frac{z^2}{c^2} = 1$$

where a, b, and c are the lengths of the semiaxes of the ellipsoid.

The canonical form of the hyperboloid of one sheet is

$$\frac{x^2}{a^2} + \frac{y^2}{b^2} - \frac{z^2}{c^2} = 1.$$

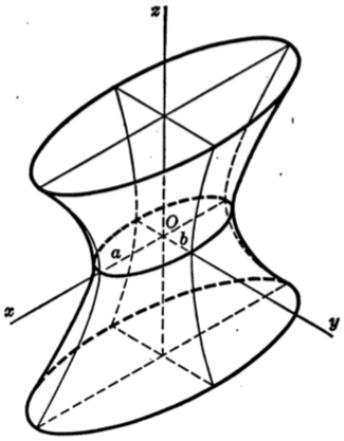

Fig. 2: Hyperboloid of one sheet, showing transverse semi-axes [3, p. 119].

The z-axis is the hyperboloid's conjugate axis (which will point along the handle's length). a and b are the lengths of the transverse semi-axes.

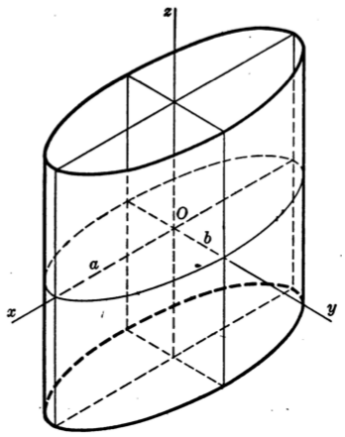

Fig. 3: Real elliptic cylinder showing transverse semi-axes [3, p. 124].

The canonical form of the real elliptic cylinder is

$$\frac{x^2}{a^2} + \frac{y^2}{b^2} = 1.$$

The z-axis is the cylinder's conjugate axis, and a and b are the lengths of the transverse semi-axes.

From [3, pp. 191-192] we also have the following two theorems:

THEOREM 1. If $f(x, y, z) = 0$ is transformed by a translation or rotation with fixed origin, the determinants and ranks of $\mathbf{q}$ and $\mathbf{Q}$ and the eigenvalues of $\mathbf{q}$ are invariant.

THEOREM 2. If $f(x, y, z) = 0$ is transformed by any coordinate or multiplying transformation, the following are invariant: the ranks of $\mathbf{q}$ and $\mathbf{Q}$, the sign of $\det \mathbf{Q}$, and whether the non-vanishing eigenvalues of $\mathbf{q}$ have the same sign.

These theorems, together with the canonical forms, yield some important properties about the centers and axes of quadric surfaces, and allow us to identify the type of quadric based on the invariant information in Theorem 2. This is explained in detail below for the three quadrics of interest; $\operatorname{rank} \mathbf{q}$, $\operatorname{rank} \mathbf{Q}$, the sign of $\det \mathbf{Q}$, and the signs of the eigenvalues of $\mathbf{q}$ have been computed for all seventeen types of quadrics [3, p. 192].

C. Quadric centers and axes

The center of a quadric is given by the following [3, p. 137]:

$$-\mathbf{q}^{-1} \begin{bmatrix} G \\ H \\ I \end{bmatrix}$$

(If $\mathbf{q}$ is rank-deficient and thus non-invertible, the quadric it represents is one of the degenerate forms, such as a cylinder or intersecting planes, that has infinitely many centers along a line or plane.)

The quadric's semi-axis lengths can be computed from the eigenvectors of $\mathbf{q}_{norm}$, where $\mathbf{q}_{norm}$ is q normalized such that the solutions to the quadric equation are given by $\mathbf{x}^T \mathbf{q}_{norm} \mathbf{x} = 1$. If the quadric's center does not coincide with the origin, this requires a change of variables $\mathbf{x}' = \mathbf{x} - \mathbf{x}_0$ (this is simply a translation, and will not change the semi-axis lengths). Letting $\mathbf{P} = \begin{bmatrix} G & H & I \end{bmatrix}^T$, this yields

$$\begin{aligned}(\mathbf{x}-\mathbf{x}_0)^T \mathbf{q} (\mathbf{x} - \mathbf{x}_0) &= (\mathbf{x} + \mathbf{q}^{-1}\mathbf{P})^T \mathbf{q} (\mathbf{x} + \mathbf{q}^{-1}\mathbf{P}) \\ &= (\mathbf{x}^T + \mathbf{P}^T \mathbf{q}^{-1}) \mathbf{q} (\mathbf{x} + \mathbf{q}^{-1}\mathbf{P}) \\ &= \mathbf{x}^T \mathbf{q} \mathbf{x} + \mathbf{P}^T \mathbf{q}^{-1} \mathbf{q} \mathbf{x} + \mathbf{x}^T \mathbf{q} \mathbf{q}^{-1} \mathbf{P} + \mathbf{P}^T \mathbf{q}^{-1} \mathbf{q} \mathbf{q}^{-1} \mathbf{P} \\ &= \mathbf{x}^T \mathbf{q} \mathbf{x} + 2\mathbf{P}^T \mathbf{x} + \mathbf{x}_0^T \mathbf{q} \mathbf{x}_0.\end{aligned}$$

Due to the quadric equation, $\mathbf{x}^T \mathbf{q} \mathbf{x} + 2\mathbf{P}^T \mathbf{x} + J = 0$, so this yields

$$(\mathbf{x} - \mathbf{x}_0)^T \mathbf{q} (\mathbf{x} - \mathbf{x}_0) = -J + \mathbf{x}_0^T \mathbf{q} \mathbf{x}_0.$$

Therefore,

$$\mathbf{q}_{norm} = \frac{\mathbf{q}}{-J + \mathbf{x_0}^T \mathbf{q} \mathbf{x_0}}.$$

The real ellipsoid is full-rank in both $\mathbf{q}$ and $\mathbf{Q}$, has $\det \mathbf{Q} < 0$, and has all positive eigenvalues. This can be seen from its canonical form:

$$\frac{x^2}{a^2} + \frac{y^2}{b^2} + \frac{z^2}{c^2} = 1$$

$$\mathbf{q} = \begin{bmatrix} A & D & E \\ D & B & F \\ E & F & C \end{bmatrix} = \begin{bmatrix} \frac{1}{a^2} & 0 & 0 \\ 0 & \frac{1}{b^2} & 0 \\ 0 & 0 & \frac{1}{c^2} \end{bmatrix}$$

$$\mathbf{Q} = \begin{bmatrix} A & D & E & G \\ D & B & F & H \\ E & F & C & I \\ G & H & I & J \end{bmatrix} = \begin{bmatrix} \frac{1}{a^2} & 0 & 0 & 0 \\ 0 & \frac{1}{b^2} & 0 & 0 \\ 0 & 0 & \frac{1}{c^2} & 0 \\ 0 & 0 & 0 & -1 \end{bmatrix}$$

The eigenvalues of $\mathbf{q}$ are thus $\frac{1}{a^2}$, $\frac{1}{b^2}$, and $\frac{1}{c^2}$. From Theorem 1, the semi-axis in the direction of an eigenvector $\vec{e}_i$ of $\mathbf{q}_{norm}$ has length $\frac{1}{\sqrt{\lambda_i}}$.

The hyperboloid of one sheet is also full-rank in both $\mathbf{q}$ and $\mathbf{Q}$, but has $\det \mathbf{Q} > 0$, and one of its eigenvalues is negative. Again, this is apparent from its canonical form.

$$\frac{x^2}{a^2} + \frac{y^2}{b^2} - \frac{z^2}{c^2} = 1$$

$$\mathbf{q} = \begin{bmatrix} A & D & E \\ D & B & F \\ E & F & C \end{bmatrix} = \begin{bmatrix} \frac{1}{a^2} & 0 & 0 \\ 0 & \frac{1}{b^2} & 0 \\ 0 & 0 & -\frac{1}{c^2} \end{bmatrix}$$

$$\mathbf{Q} = \begin{bmatrix} A & D & E & G \\ D & B & F & H \\ E & F & C & I \\ G & H & I & J \end{bmatrix} = \begin{bmatrix} \frac{1}{a^2} & 0 & 0 & 0 \\ 0 & \frac{1}{b^2} & 0 & 0 \\ 0 & 0 & -\frac{1}{c^2} & 0 \\ 0 & 0 & 0 & -1 \end{bmatrix}$$

The eigenvalues of $\mathbf{q}$ are $\frac{1}{a^2}$, $\frac{1}{b^2}$, and $-\frac{1}{c^2}$. Thus, the conjugate axis of any hyperboloid of one sheet is the eigenvector of $\mathbf{q}_{norm}$ corresponding to the negative eigenvalue, and the lengths of the transverse semi-axes can be found from the other two eigenvalues.

The real elliptic cylinder has $\operatorname{rank} \mathbf{Q} = 3$ and $\operatorname{rank} \mathbf{q} = 2$, and exactly one zero eigenvalue; the other eigenvalues are positive. It has $\det \mathbf{Q} < 0$.

$$\frac{x^2}{a^2} + \frac{y^2}{b^2} = 1$$

$$\mathbf{q} = \begin{bmatrix} A & D & E \\ D & B & F \\ E & F & C \end{bmatrix} = \begin{bmatrix} \frac{1}{a^2} & 0 & 0 \\ 0 & \frac{1}{b^2} & 0 \\ 0 & 0 & 0 \end{bmatrix}$$

$$\mathbf{Q} = \begin{bmatrix} A & D & E & G \\ D & B & F & H \\ E & F & C & I \\ G & H & I & J \end{bmatrix} = \begin{bmatrix} \frac{1}{a^2} & 0 & 0 & 0 \\ 0 & \frac{1}{b^2} & 0 & 0 \\ 0 & 0 & 0 & 0 \\ 0 & 0 & 0 & -1 \end{bmatrix}$$

One of the eigenvalues of $\mathbf{q}$ is zero, corresponding to the eigenvector pointing along the cylinder's axis. The other two eigenvalues, as before, are positive, and the ellipse's semi-axes can be computed from them if the coefficients are properly normalized. To find $\mathbf{q}_{norm}$ for the cylinder, since $\mathbf{q}$ is not invertible and no single center exists, we take as center an arbitrary point along the cylinder's axis.

The centers, axis vectors, and semi-axis lengths of these quadric surfaces will be used to identify and classify handle-like affordances.

IV. Handle Identification Pipeline

The handle identification pipeline is similar to that in [2]. The input is a segmented point cloud corresponding to an object. This point cloud is then voxelized and surface normals found, using the method given in [4]. Points are then randomly sampled from the cloud; these are the centers of *neighborhoods*, which are cube-shaped subsets of the point cloud.

Quadric fitting is done using the approximate method given in [5]. This method makes use of the surface normals to fit quadrics more efficiently than previous methods. The quadric fit is tested against various criteria for being "handle-shaped", and if it passes, the neighborhood is selected as a candidate handle location.

A. Handle Criteria

If the quadric representing a handle is not categorized as a cylinder, ellipsoid, or hyperboloid of one sheet, it is rejected. The center of an ellipsoid or hyperboloid of one sheet is required to be close to the neighborhood's center, else the quadric is likely non-representative of the object's surface. Since a cylinder does not have a center, the projection distance from the neighborhood's center to the cylinder's axis is tested instead. Finally, the smallest semi-axis of the ellipsoid, or smaller transverse semi-axis of the hyperboloid or cylinder, must not exceed half of the maximum possible grasp width.

Future work could test whether further restrictions improve the handle detection accuracy: for example, requiring the ellipsoid to have a certain minimum eccentricity (to exclude ellipsoids that are too much like spheres), or applying a grasp-width test to the larger semi-axis perpendicular to the handle's axis.

B. Visualization

Since the general quadric equation is an implicit equation (of the form $f(x, y, z) = 0$) rather than an explicit equation (of the form $z = f(x, y)$), quadrics can be challenging to plot and visualize. For debugging purposes, a simple visualizer was used that samples points in the area of interest and checks that $|f(x, y, z)| \leq \epsilon$. This was conceptually simple, but was slow to run unless the point resolution was very low, and at a low point resolution some features of the quadrics (for example, hyperboloids of one sheet vs. hyperboloids of two sheets) became difficult to distinguish.

Recent work has provided a useful two-variable quadric parameterization that can be used for visualization [6]. However, this parameterization requires the quadric to intersect the origin, so that $J = 0$. Computing the required offset for the fully general quadric equation seemed unnecessarily complex, so it is done based on the quadric type; currently this is only implemented for the ellipsoid and hyperboloid of one sheet.

V. Results

The quadric-fit algorithm works well, and the quadrics it produces appear to be a good fit to the input point cloud.

The handle detector has been tested on selected point clouds from the YCB dataset [7]. The original goal of testing on real point clouds proved infeasible, so noise has been added to some of the YCB point clouds to simulate an imperfectly collected point cloud.

A. Performance on YCB point clouds without added noise

A subset of objects with suitable handles were selected from the YCB dataset: the chips can and lemon from the food items category, the mug, spatula, and fork from kitchen items, and the power drill, flat-head screwdriver, and hammer from tool items. The number of neighborhoods sampled from the object was based on the size of the object as measured by the number of points in the voxelized point cloud. Detection accuracy was computed as the percent of neighborhood centers labeled as handles that fell in an actual handle region [2].

	Chips	Lemon	Mug	Spatula	Fork	Drill	Screwdriver	Hammer
Accuracy	1.0	0.97	0.0	1.0	1.0	0.29	1.0	0.53

TABLE I: Detection accuracy for all objects with no noise.

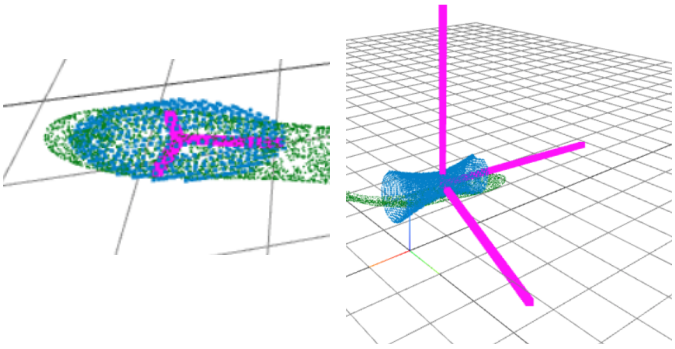

Fig. 4: Ellipsoid and hyperboloid fitted to spatula handle, with axes shown. Ellipsoid's axes have been scaled to correct semi-axis lengths.

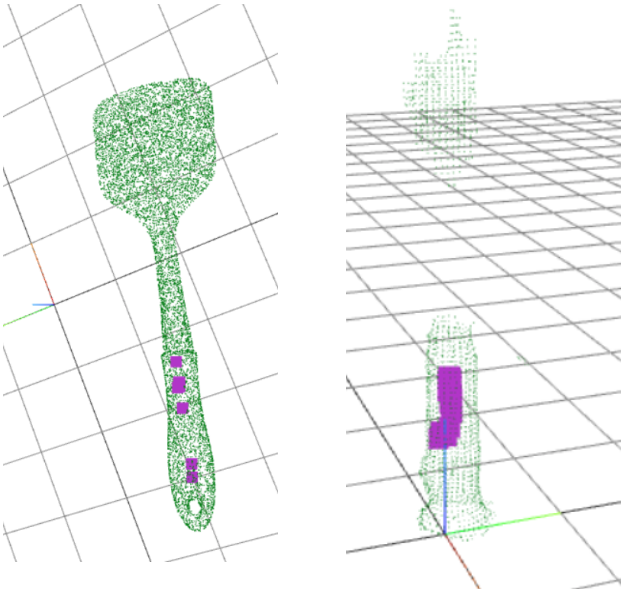

Fig. 5: Successful handle detections: fork and spatula

The mug, drill, and hammer performed poorly, but all other objects selected achieved high detection accuracy rates. The first row of table I gives the detection accuracies for one trial of the pipeline, with no added noise. The mug, drill, and hammer all have fairly cylindrical non-handle regions, which were falsely detected as handles. In addition, the trigger region of the drill and the claw region of the hammer were sufficiently concave that handle-like quadrics were fitted to the outside of the object.

B. Performance on YCB point clouds with added noise

Various amounts of noise were then added to the point clouds that the handle detector performed well on. Noise was

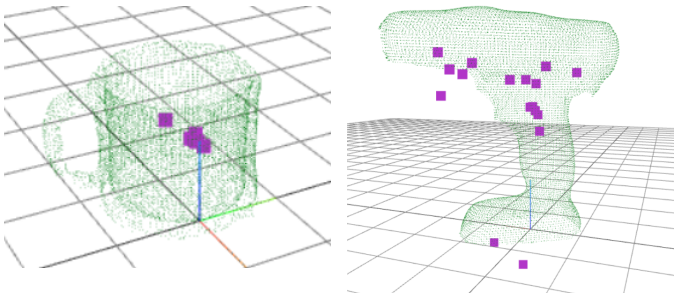

Fig. 6: Unsuccessful handle detections: mug and drill

generated by multiplying all points in the point cloud by a random amount with mean 1.0 and standard deviation σ.

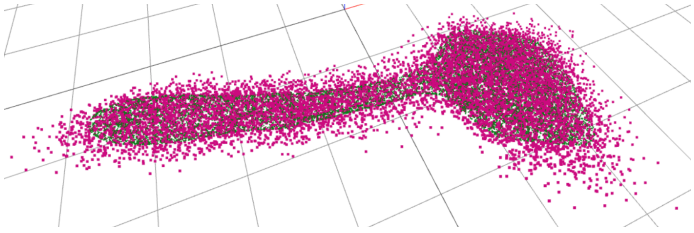

Fig. 7: Original spatula (green), spatula with $\sigma = 0.1$ noise (pink).

σ	Chips	Lemon	Spatula	Fork	Screwdriver
0.0	0.86	1.0	0.71	1.0	1.0
0.01	1.0	1.0	1.0	0.67	1.0
0.02	1.0	1.0	0.57	1.0	1.0
0.03	1.0	1.0	0.66	1.0	1.0
0.04	1.0	1.0	0.4	0.83	1.0
0.05	1.0	1.0	0.75	0.67	1.0
0.06	1.0	1.0	0.0	0.75	1.0
0.07	1.0	1.0	1.0	1.0	1.0
0.08	1.0	1.0	1.0	0.67	1.0
0.09	0.0	1.0	0.0	1.0	0.78
0.1	1.0	1.0	1.0	1.0	0.8

TABLE II: Detection accuracy for some objects with various amounts of noise.

Table II gives the detection accuracies as a function of noise for each object. Since the pipeline was only run once for each combination of σ and object, and the randomness of the samples is a significant factor in the pipeline's success, these results are erratic, but still suggestive.

Most of the errors were due to handles being fitted to the outside of the object. With noise, the spatula seems to be particularly susceptible to this. To improve the handle detector, an additional heuristic should be developed (perhaps using the normals) to reject quadric centers outside the object. The number of detected handle centers also seemed to decrease with added noise.

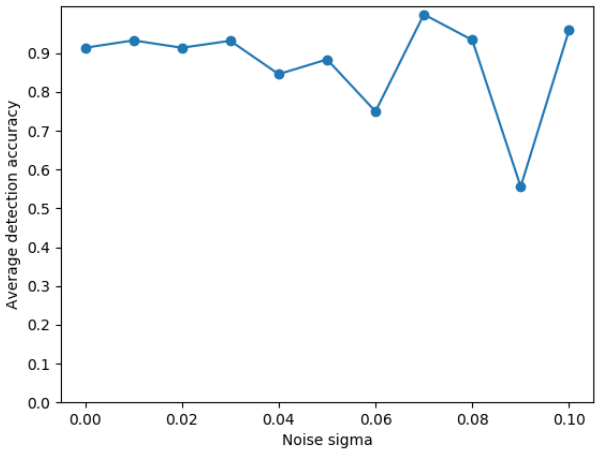

Fig. 8: Detection accuracy, averaged over objects, as a function of σ.

C. Benchmarks

For most robotics applications, it is necessary for perception tasks to operate in real time. There is somewhat more leeway with grasping objects than with many other applications, but it is nevertheless desirable that the robot not waste too much time pondering possible grasps.

Step	Time (s)
Voxelization	0.10
Computing normals	39.6
Sampling one neighborhood (average)	0.11
Sampling 40 neighborhoods	4.35
Fitting one quadric (average)	0.003
Fitting 40 quadrics	0.13
Handle checking one quadric (average)	0.00025
Handle checking 40 quadrics	0.010

TABLE III: Duration of each step of pipeline for spatula

As Table III demonstrates, by far the most time-consuming part of the pipeline is computing surface normals for the point cloud. The cost of the quadric-fitting step is comparatively modest. Since surface normals are computed using the code from [4], and neighborhood sampling is done using a naive approach linear in both the number of points in the point cloud and the number of neighborhoods to sample, both of these steps could potentially be made more efficient.

D. Comparison to Prior Work

The method presented in [2] improves on pure quadric fitting in several ways: first, a shell of some thickness is added around the fitted cylinder, and handle candidates with too many points inside this shell are rejected. This could, for example, help reject some of the false handles detected on the hammer's head and claws, since the hammer handle would lie within this shell. Second is the technique presented for occlusion filtering. This is based on the specific geometry of the depth-camera setup, and was not necessary in this case since none of the YCB objects are occluded.

The quadric fitting method used in [2] also does not require surface normals, which represent most of the total duration of the handle detection pipeline. However, many other grasping and object perception operations also require surface normals, so if handle detection is performed alongside these operations, reusing the surface normals requires no additional computation.

VI. Future Work

The original intent of this project was to test the performance of handle detection by quadric fitting on point clouds collected from the 6.881 robot setup, and compare this method to the performance of other handle-detection methods currently in use. Although I was unable to collect these "real" point clouds, I believe this would still be a useful line of inquiry.

Additionally, it might be interesting to explore adjustments mentioned earlier in the paper that could improve performance. In particular, additional criteria could be placed on candidate handle quadrics, such as an ellipsoid eccentricity test, a minimum grasp width test, or the shell test from [2]. It is also desirable to restrict handle centers to lie inside the object, which should be possible to compute from surface normals; further testing is necessary to check the computational feasibility of this method.

VII. Conclusion

While this method does not work on all objects with handles (in particular objects such as mugs where the handle is not very quadric-shaped, or such as the electric drill, where quadric shapes exist on non-handle parts of the object), it achieves good results on others, with reasonable robustness to noise. The quadric-fit algorithm is based on the object's surface normals, which are often generated in the course of other grasping operations, and quadric fitting itself is quite fast. Overall, this method is a useful addition to the broader arsenal of handle detection methods.

References

[1] R. A. Gutierrez, "Learning task-oriented grasp heuristics from demonstration," Master's thesis, MIT, 2016.

[2] A. ten Pas and R. Platt, "Localizing grasp affordances in 3-D point clouds using Taubin quadric fitting," *CoRR*, vol. abs/1311.3192, 2013. [Online]. Available: http://arxiv.org/abs/1311.3192

[3] J. M. H. Olmsted, *Solid Analytic Geometry*. New York, NY: D. Appleton-Century Company, 1947.

[4] 6.881 Staff. (2019) Problem set 3, part 2. [Online]. Available: http://manipulation.csail.mit.edu/pset3/pset3_robust_perception.html

[5] T. Birdal, B. Busam, N. Navab, S. Ilic, and P. Sturm, "A minimalist approach to type-agnostic detection of quadrics in point clouds," in *2018 IEEE/CVF Conference on Computer Vision and Pattern Recognition*, 2018, pp. 3530–3540.

[6] C. Zhang and C. Zhang, "A simple method for the parameterization of quadric surfaces," in *2009 International Conference on Information Engineering and Computer Science*, 2009, pp. 1–4.

[7] B. Calli, A. Singh, J. Bruce, A. Walsman, K. Konolige, S. Srinivasa, P. Abbeel, and A. M. Dollar, "Yale-CMU-Berkeley dataset for robotic manipulation research," *The International Journal of Robotics Research*, vol. 36, no. 3, pp. 261–268, 2017. [Online]. Available: https://doi.org/10.1177/0278364917700714